

UDC 629.705

DOI: <https://doi.org/10.20535/0203-3771432022275282>

O. V. Zbrutsky¹, *Doc. of Science, professor*, **V. V. Meleshko²**, *PhD, associate professor*, **A. P. Ganja³**, *PhD, senior researcher*, **S. V. Tarnavsky⁴**, *PhD, senior researcher*, **O. M. Bondarenko⁵**, *PhD, associate professor*, **S. O. Ponomarenko⁶**, *PhD, associate professor*, **K. Saurova⁷**, *senior lecture*

SYSTEM DEFINITION OF MICRO- NANO SATELLITE ORIENTATION

Ua

Розглядається задача побудови системи визначення орієнтації мікро та нано супутника з врахуванням можливості її імплементації використанням існуючих сенсорів. На основі аналізу існуючих методів та авторських досліджень сформована методика побудови системи визначення орієнтації. Вона включає послідовність формування розрахункових значень фізичних полів в необхідних системах координат, значень сигналів сенсорів фізичних полів та алгоритму триад для розрахунку кутів орієнтації. Наведені основні технічні характеристики сенсорів фізичних полів, які можуть бути використані для реалізації розглянутої методики визначення орієнтації супутників класу CubeSat.

En

The task of building a system for determining the orientation of micro and nano satellites is considered, taking into account the possibility of its implementation and the use of existing sensors. Based on the analysis of existing methods and author's research, a methodology for building a system for determining orientation was formed. It includes the sequence of formation of calculated values of physical fields in the necessary coordinate systems, signal values of sensors of physical fields and the triad algorithm for calculating orientation angles. The main technical characteristics of sensors of physical fields, which can be used to implement the considered technique for determining the orientation of CubeSat class satellites, are given.

Introduction

A significant amount of theoretical research is devoted to the tasks of determining the orientation of microsatellites in the overwhelming majority. Magnetic control is considered in detail. A completely magnetic orientation system has not yet been tested in flight, and research is far from complete [1]. In [2] a

¹ Igor Sicorskyi Kyiv Politechnical Institute

² Igor Sicorskyi Kyiv Politechnical Institute

³ Igor Sicorskyi Kyiv Politechnical Institute

⁴ Igor Sicorskyi Kyiv Politechnical Institute

⁵ Igor Sicorskyi Kyiv Politechnical Institute

⁶ Igor Sicorskyi Kyiv Politechnical Institute

⁷ Almaty University of Energy and Communications

fairly complete overview of magnetic orientation algorithms is given. Magnetic orientation systems of small satellites are considered. The field of application of active magnetic orientation systems is noticeably wider than that of passive systems. Approaches to the development of the microsatellite orientation system are outlined in [2, 3, 4]. The satellite orientation system does not have strict requirements for ensuring its angular movement. In [5], a miniaturized orientation control system suitable for nanosatellites is described and designed using only commercial off-the-shelf components to integrate this system into nanosatellites such as Cubesats. Orientation determination using local algorithms is discussed in [6], and recursive algorithms based on measurements of orientation sensors and the movement model of the device are shown in [7, 8].

Practical uses of microsatellite orientation algorithms are given for only a few microsatellites. There are no practical recommendations for the use of algorithms. Active systems make it possible to implement any orientation within the limits of their resources, to ensure high accuracy of orientation and high speed at the cost of increasing complexity, volume, mass and cost. This significantly limits the possibility of using such systems for small satellites.

Formulation of the problem

Will consider the methodology of the approach and the method of building a system for determining the orientation of micro and mini satellites and the existing technical means of their implementation.

Main results. Coordinate systems

1. Earth-Centered Inertial frame coordinate system $OX_iY_iZ_i$ (ECI) – system with the beginning in the center of the Earth (Fig. 1) [9]. The X_i axis is located in the plane of the equator and is directed to the vernal equinox. The Y_i axis is located in the plane of the equator and complements the coordinate system to the right. The Z_i axis is perpendicular to the plane of the equator and is directed along the axis of rotation of the Earth.

Spacecraft (SC) motion parameters in the ECI: $\bar{r}_i = [x_i \quad y_i \quad z_i]^T$ – radius-vector of the center of mass of the SC, $\bar{V}_i = [V_{xi} \quad V_{yi} \quad V_{zi}]^T$ – vector of the absolute velocity of the center of mass of the SC.

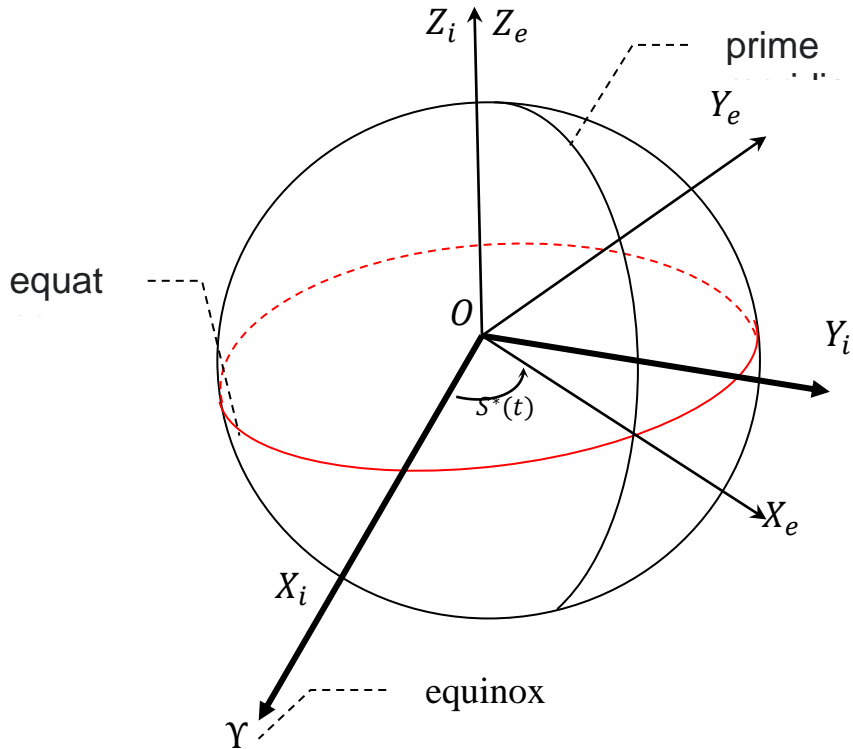


Fig. 1. Earth-Centered Inertial coordinate system

2. Earth-Centered Earth-Fixed (Earth's geocentric) frame coordinate system (ECEF) $OX_eY_eZ_e$ [9] – a coordinate system rigidly linked to the Earth and with the beginning at its center. Axis X_e is located in the plane of the equator and passes through the point of intersection of the equator and the Greenwich (zero) meridian. Axis Y_e complements the system to the right. Axis Z_e perpendicular to the plane of the equator and directed along the axis of rotation of the Earth. Rotation in the plane of the equator between ECI i ECEF given by the angle [10] (Fig. 2)

$$S^*(t) = S_0(t_0) + \Omega_3 \cdot \Delta t,$$

where $\Omega_3 = 7292115 \cdot 10^{-11} \left[\frac{\text{rad}}{\text{sec}} \right]$ – angular velocity of the Earth rotation around its own axis [11, 12]; $S_0(t_0)$ – Sidereal time [rad] at a given time; $\Delta t = t - t_0$ – UTC time [sec] from the moment of definition $S_0(t_0)$.

Parameters of the SC in ECEF $\vec{r}_e = [x_e \ y_e \ z_e]^T$ – the radius-vector of the center of mass of the SC (M is the subsatellite point of the center of mass), λ – geocentric longitude; φ – geocentric latitude (Fig. 2).

The connection between the ECI and ECEF coordinate systems is determined by the equation

$$[x_i \ y_i \ z_i]^T = C_1 \cdot [x_e \ y_e \ z_e]^T, \quad (1)$$

$$C_1 = \begin{bmatrix} \cos S^* & -\sin S^* & 0 \\ \sin S^* & \cos S^* & 0 \\ 0 & 0 & 1 \end{bmatrix}.$$

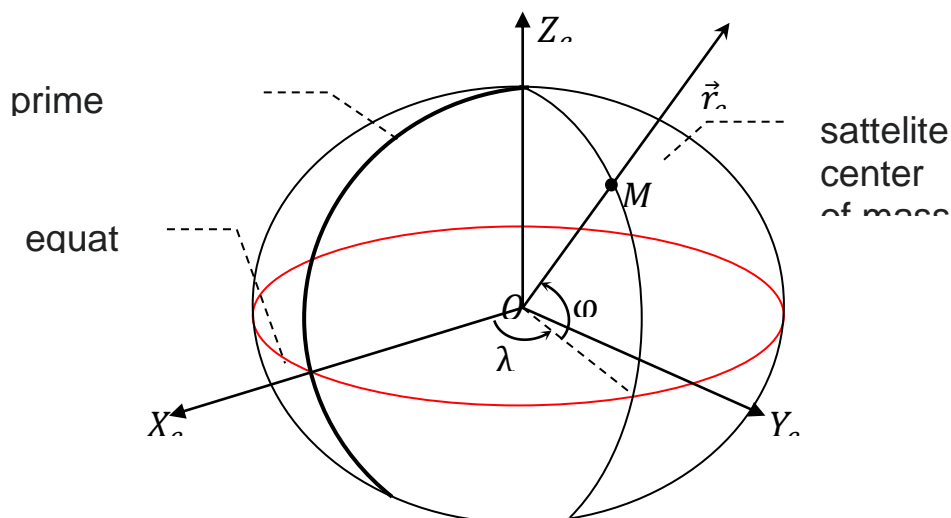


Fig. 2. Earth-Centered Earth-Fixed coordinate system

3. Orbital satellite coordinate system $X_o Y_o Z_o$ (OSCS) (Fig. 3) with the beginning at the center of mass of the SC. Axes X_o and Z_o lies in the plane of the SC's orbit. Axis Z_o is a continuation of the SC's radius-vector \vec{r}_i . Axis X_o is perpendicular to the axis Z_o and for the circular orbit of the SC coincides in direction with the SC's absolute velocity vector $\vec{V}_i = \vec{V}_e$. Axis Y_o complements the coordinate system to the right.

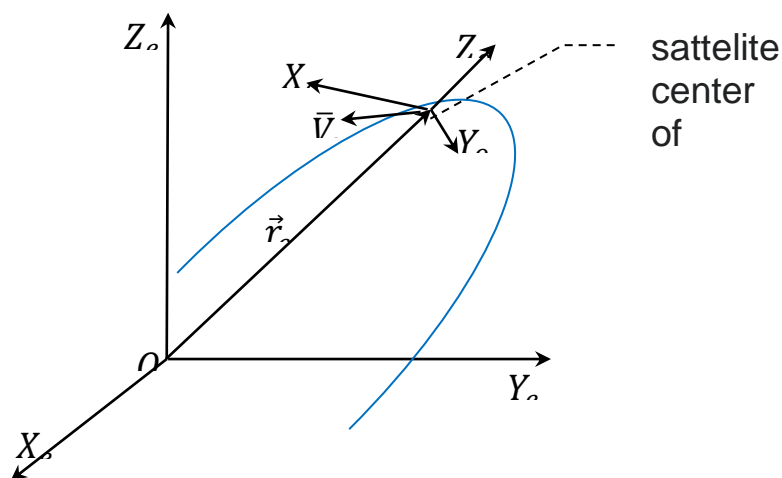


Fig. 3. Orbital satellite coordinate system

The direction cosines of the OSCS orts in the ECEF:

$$\begin{aligned} z_o &= \frac{\bar{r}_e}{|\bar{r}_e|} = [z_{Xe} \quad z_{Ye} \quad z_{Ze}]^T, \\ y_o &= \frac{\bar{r}_e \times \bar{V}_e}{|\bar{r}_e \times \bar{V}_e|} = [y_{Xe} \quad y_{Ye} \quad y_{Ze}]^T, \\ x_o &= y_o \times z_o = [x_{Xe} \quad x_{Ye} \quad x_{Ze}]^T. \end{aligned} \quad (2)$$

4. Orbital geographic coordinate system (OGCS) $X_g Y_g Z_g$ (Fig. 4), where axis X_g is in the plane of the meridian and is perpendicular to the SC's radius-vector r and directed in the northern direction, the axis Y_g is directed to the west and complements the coordinate system to the right, axis Z_g is a continuation of the radius-vector r of the SC's center of mass. The connection of OSCS and OGCS is determined by the equation

$$\begin{aligned} [x_g \quad y_g \quad z_g]^T &= C_2 \cdot [x_o \quad y_o \quad z_o]^T, \\ C_2 &= \begin{bmatrix} \cos A & -\sin A & 0 \\ \sin A & \cos A & 0 \\ 0 & 0 & 1 \end{bmatrix}, \end{aligned} \quad (3)$$

where A – the azimuth of the orbit at a given time, $\sin A = \frac{\cos i}{\cos \varphi}$,

$\cos A = \frac{\cos u}{\cos \varphi} \cdot \sin i$ [10], i – the orbit inclination, u – the orbit argument of the

latitude at a given time.

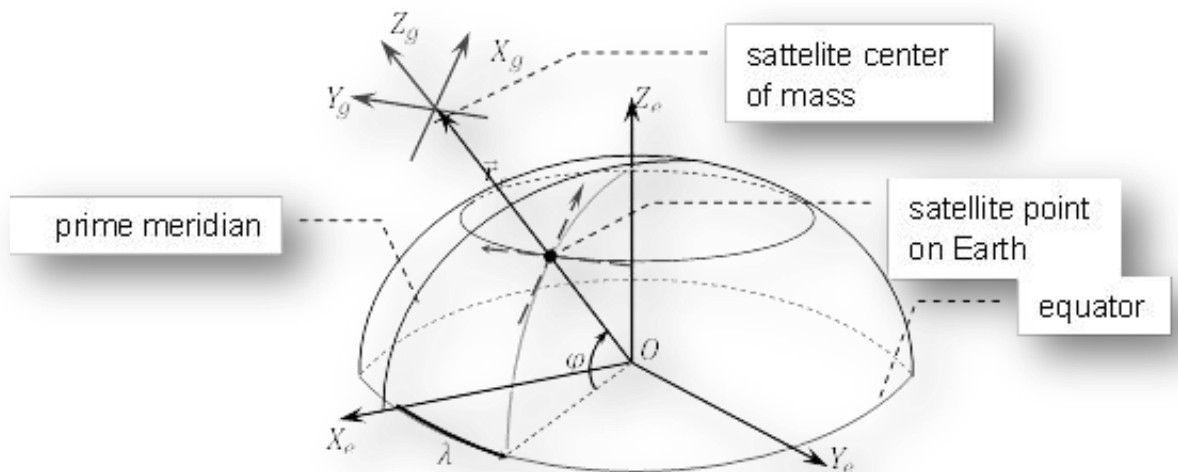


Fig. 4. Orbital geographic coordinate system

The connection of OGSC and ECEF is determined by the equation

$$\begin{bmatrix} x_g & y_g & z_g \end{bmatrix}^T = C_3 \begin{bmatrix} x_e & y_e & z_e \end{bmatrix}^T, \quad (4)$$

where

$$C_3 = \begin{bmatrix} -\cos \lambda \cdot \sin \varphi & \sin \lambda & -\cos \lambda \cdot \cos \varphi \\ -\sin \lambda \cdot \sin \varphi & -\cos \lambda & -\sin \lambda \cdot \cos \varphi \\ -\cos \varphi & 0 & \sin \varphi \end{bmatrix}.$$

5. Body coordinate system (BCS) $X_b Y_b Z_b$ (Fig. 5) – a coordinate system rigidly connected with the satellite, the position of which in space can be given by the Euler-Krylov angles ψ, θ, γ in OGCS.

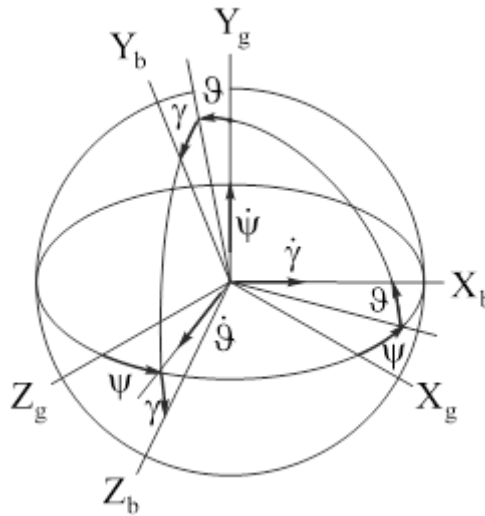


Fig. 5. Body coordinate system

The connection between BCS and OGCS is given by the equation

$$\begin{bmatrix} x_b & y_b & z_b \end{bmatrix}^T = C_4 \begin{bmatrix} x_g & y_g & z_g \end{bmatrix}^T, \quad (5)$$

where

$$C_4 = \begin{bmatrix} \cos \psi \cos \vartheta & \sin \vartheta & -\sin \psi \cos \vartheta \\ \sin \psi \sin \gamma - \cos \psi \cos \gamma \sin \vartheta & \cos \vartheta \cos \gamma & \cos \psi \sin \gamma + \sin \psi \cos \gamma \sin \vartheta \\ \sin \psi \cos \gamma + \cos \psi \sin \gamma \sin \vartheta & -\cos \vartheta \sin \gamma & \cos \psi \cos \gamma - \sin \psi \sin \gamma \sin \vartheta \end{bmatrix}$$

Parameters of the Sun in the inertial geocentric equatorial coordinate system (ECI). The longitude of the Sun is determined by the expression [9, 13]

$$\lambda_{\square} = \text{rem} \left[0,7859453 + \frac{M_{\square}}{2\pi} + (6893,0 \cdot \sin M_{\square} + 72,0 \cdot \sin(2 \cdot M_{\square})) + 6191,2 \cdot T) / s_{2\pi} \right] \cdot 2\pi,$$

where $M_{\square} = \text{rem}[0,993133 + 99,997361 \cdot T] \cdot 2\pi$, $\text{rem}[\dots]$ – the function of extracting the fractional part of a number, for example $\text{rem}[1,2]=0,2$,

$s_{2\pi} = 1296000$ – number of arcseconds from 0 до 2π , $T = \frac{d_{2000}}{36525}$ – the number of centuries since the epoch 2000,0 to 0^h settlement date, $d_{2000} = JD(t) - J2000,0$ – number of days since 01.01.2000 (moment in time 12:00 January 1, 2000, which is considered the beginning of the Julian era J2000.0) to the settlement date, $JD(t)$ – the Julian day number for the given time t (Gregorian date + UTC) [9, 13],

$$JD(t) = JD_N + \frac{hh - 12}{24} + \frac{mm}{1440} + \frac{ss.sss}{86400},$$

dd.MM.yyyy і hh:mm:ss.sss – current Gregorian date and UTC time (yyyy – year number of the Gregorian calendar, MM – the number of the month of the Gregorian calendar in the year, dd – Gregorian calendar day number in month, UTC time: hh – hours, mm – minutes, ss.sss – seconds and second's fractions); JD_N – whole meaning of Julian day

$$JD_N = dd + \text{int} \left[\frac{153 \cdot m + 2}{5} \right] + 365 \cdot y + \text{int} \left[\frac{y}{4} \right] - \text{int} \left[\frac{y}{100} \right] + \text{int} \left[\frac{y}{400} \right] - 32045,$$

$$a = \text{int} \left[\frac{14 - MM}{12} \right], \quad y = yyyy + 4800 - a, \quad m = MM + 12 \cdot a - 3,$$

“ $\text{int}[\dots]$ ” – the function of selecting an integer part of a number.

The angle of inclination of the ecliptic to the earth's equator

$$\varepsilon_A = \left(84381,448 + (-46,8150 + (-0,00059 + 0,001813 \cdot T) \cdot T) \cdot T \right) / s_{rad},$$

$s_{rad} = 3600 \cdot 180 / \pi$ – conversion factor in radians.

The direction cosines of the Sun's unit vector [13, 14]

$$\begin{aligned} S_{xi} &= \cos \lambda_{\varepsilon_{\square}} \\ S_{yi} &= \sin \lambda_{\varepsilon_{\square}} \cdot \cos \varepsilon_A \\ S_{zi} &= \sin \lambda_{\varepsilon_{\square}} \cdot \sin \varepsilon_A. \end{aligned} \quad (6)$$

The Earth's magnetic field model. In the orbital geographic coordinate system (Fig. 6) we have:

On the Fig. 6: B – the Earth's magnetic field (EMF) induction vector; B_{x_g} , B_{y_g} , B_{z_g} – geographic northern, eastern and lower components of the magnetic induction vector. Geographic components of the magnetic field at a given point with coordinates λ, φ, r for a given moment in time t , are calculated by formulas [15, 16, 17]

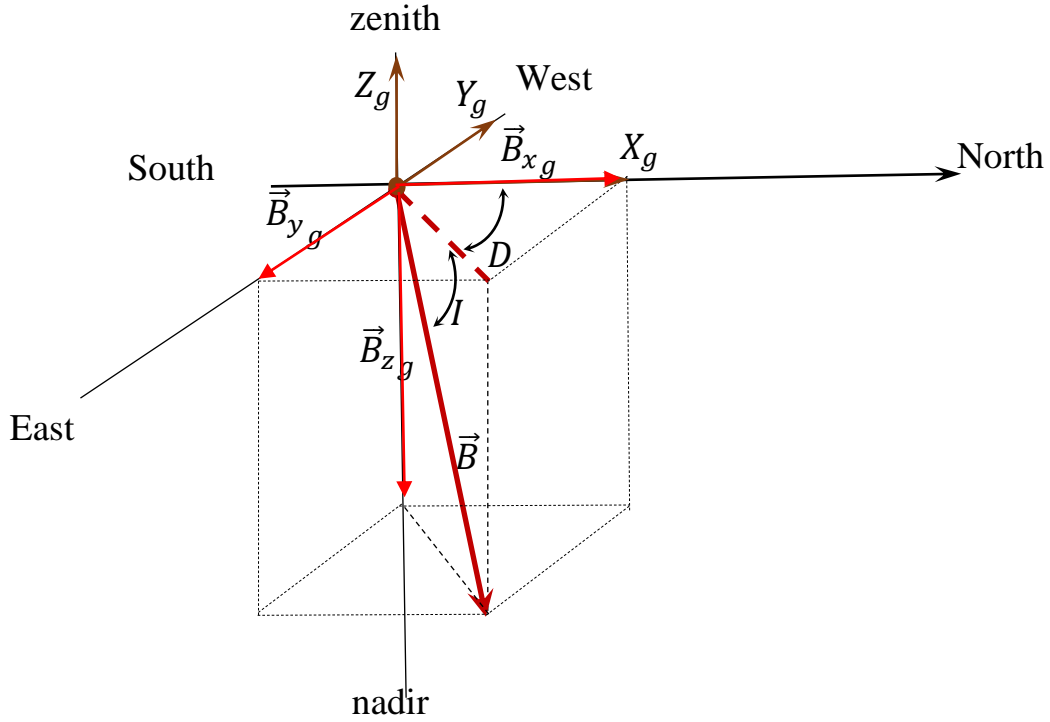


Fig. 6. Earth's magnetic field induction vector

$$\begin{aligned}
 B_{x_g} &= -\sum_{n=1}^N \left(\frac{a}{r}\right)^{n+2} \sum_{m=0}^n \left[\hat{g}_n^m(t) \cdot \cos(m \cdot \lambda) + \hat{h}_n^m(t) \cdot \sin(m \cdot \lambda) \right] \cdot \frac{dP_n^m \sin \varphi}{d\varphi}, \\
 B_{y_g} &= -\frac{1}{\cos \varphi} \sum_{n=1}^N \left(\frac{a}{r}\right)^{n+2} \sum_{m=0}^n m \left[\hat{g}_n^m(t) \cdot \sin(m \cdot \lambda) - \hat{h}_n^m(t) \cdot \cos(m \cdot \lambda) \right] \times \\
 &\quad \times P_n^m \sin \varphi, \\
 B_{z_g} &= \sum_{n=1}^N (n+1) \cdot \left(\frac{a}{r}\right)^{(n+2)} \sum_{m=0}^n \left[\hat{g}_n^m(t) \cdot \cos(m \cdot \lambda) + \hat{h}_n^m(t) \sin(m \cdot \lambda) \right] \cdot P_n^m \sin \varphi,
 \end{aligned} \tag{7}$$

where $\hat{g}_n^m(t), \hat{h}_n^m(t)$ – un normalized Gaussian coefficients.

Parameters of stars in the inertial geocentric equatorial coordinate system. The direction cosines of the star's unit vector [19]

$$\begin{aligned}
 K_{x_i} &= \cos \delta^* \cos \alpha^*, \\
 K_{y_i} &= \cos \delta^* \sin \alpha^*, \\
 K_{z_i} &= \sin \delta^*,
 \end{aligned} \tag{8}$$

where δ^* – elevation angle, α^* – right ascension angle is star's spherical coordinates.

Algorithms for determining satellite orientation by the Earth's magnetic field and celestial bodies

The algorithms of the orientation determination system are designed for interaction with external information and measurement sensors and systems: the receiver of the global satellite navigation system, the Sun sensor, the magnetometer, the starry sky sensor. Let's consider the most common sensors of orientation systems of micro and nano satellites.

Global Navigation Satellite System (GNSS) receiver. Specialized receiver (GNSS) type ACH-5206 designed to receive signals from GNSS groups of navigation satellites on board the Earth's artificial satellites, their processing on the built-in microcontroller and determination of the exact time, angular or linear geographic coordinates, altitude, components of the satellite's linear speed and provides the characteristics specified in Tab. 1 [19].

Table 1.

Main technical characteristics of the GNSS receiver type ACH-5206

Working signals	GPS, GALILEO, GLONASS, SBAS
Measurement range:	
Height	till 50 thousands km
Speed	till 10000 m/s
Acceleration	till 50 g
Geographic coordinates	latitude ± 90 deg /longitude ± 180 deg
Frequency of issuing signals	1, 2, 5, 10 Hz
Definition error (3σ):	
–on the surface coordinates	< 8 m
– height coordinates	< 10 m
–velocity	< 0,05 m/s
–time	< 45 ns

Two-coordinate sensor of the Sun. Compact solar sensor type nanoSSOC A-60 is the most common model used on small CubeSat-type satellites. The sensor is two-coordinate, has four matrix photocells with an analog output, the signals of which are transmitted through an external ADC to a peripheral microcontroller for processing [20]. The deviation angles of the direction vector to the Sun in two orthogonal planes that pass through the normal to the photocell plane and the sensitivity axis are calculated by the microcontroller using the manufacturer's factory program using LUT photocell sensitivity calibration tables. The main characteristics of the Sun sensor are listed in Tab. 2.

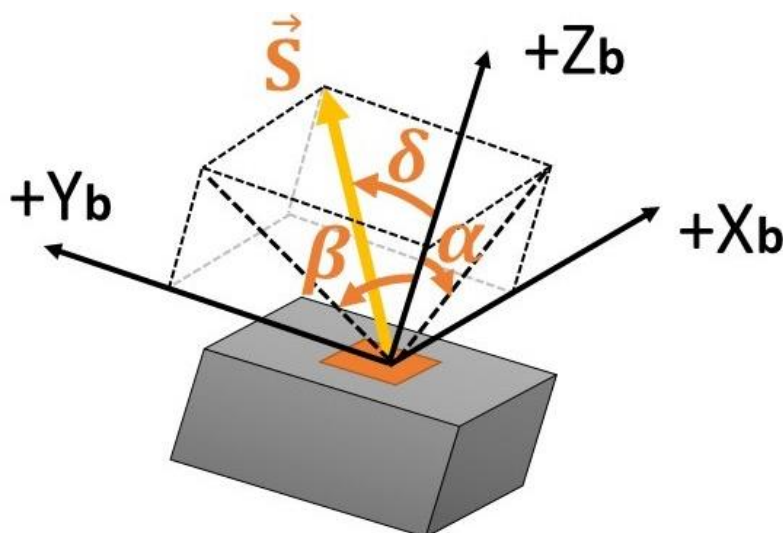
At the output of the solar sensor signal processing program, information is generated about the measured angles, or about the error code, if one of the failure options has occurred.

Table 2.

Main technical characteristics of the nanoSSOC A-60
two-coordinate Sun sensor

sight field	± 60 deg
unobstructed deflection field	± 75 deg
sensitivity	$< 0,1$ deg
total error the root mean square deviation (3σ)	$< 0,5$ deg

Two-coordinate Sun sensor mathematical model. A common type of solar sensor for nano- and micro-satellites is a two-coordinate sensor with four sensitive elements (photodiode arrays), which allows you to determine two angles of deviation of the light flux from the normal to the plane of the photodiodes in two mutually perpendicular planes, as shown in Fig. 7 [20]. Output analog signals of sensitive elements are sent through the ADC to the peripheral microcontroller, which, according to the program of the sensor manufacturer, calculates and outputs the values of the output angles α i β , if the Sun is in the FoV.

Fig. 7. Diagram of output angles α , β two-coordinate Sun sensor

Projections of the unit vector \vec{S} on the axis BCS (Fig. 7) will look like

$$S_{x_b} = \cos \delta \tan \alpha, \quad S_{y_b} = \cos \delta \tan \beta, \quad S_{z_b} = \cos \delta, \quad (9)$$

where δ – the angle of incidence of solar radiation on the plane of the photocells of the sensor. Since within the field of vision of the sender $0 \leq \delta \leq \text{FoV}$, formulas can be used to generate output signals

$$\alpha = \tan^{-1}(S_{x_b} / S_{y_b}) + \Delta\alpha, \quad \beta = \tan^{-1}(S_{y_b} / S_{z_b}) + \Delta\beta, \quad (10)$$

$$\delta = \tan^{-1} \sqrt{\tan^2 \alpha + \tan^2 \beta},$$

where $\Delta\alpha$ and $\Delta\beta$ – sensor errors.

Algorithm of operation of the 6-component Sun sensor

Often, for CubeSat satellites, six orthogonally oriented two-coordinate solar sensors are used, installed on each face of the satellite so that the axes are parallel to the BCS axes and uniformly cover the surrounding space [21]. If SV_j is a vector of unit vector component values \vec{S} direction to the Sun, measured by the j -th sensor ($j=1\dots 6$) in the axes BCS,

$$SV_j = [S_{xj} \quad S_{yj} \quad S_{zj}],$$

where S_{xj} , S_{yj} , S_{zj} – values calculated by formula (8) according to the values of the measured angles α_i , β_i and the calculated angle δ_i (9) for the j -th sensor, then the evaluation of the components of the Sun vector SEB in BCS

$$SEB = [SEB_x \quad SEB_y \quad SEB_z]$$

from the signals of all six sensors, we determine by the method of the simple average value of the sum of the vectors SV_j reduced to BCS:

$$SEB = \left(\sum_{j=1}^6 MSB_j \cdot SV_j^T \right) / \left| \sum_{j=1}^6 MSB_j \cdot SV_j^T \right|,$$

where MSB_j – rotation matrix from j -th sensors axes to BCS.

This algorithm makes it possible to determine the estimates of the components of the Sun vector in BCS and for a smaller number of sensors.

Three-component magnetometer. It is designed to measure the three orthogonal components of the magnetic induction vector of the Earth's magnetic field in low-Earth orbits. It includes six HMC1001 high-resolution analog sensors installed in pairs along three measuring axes, an ADC module and a microcontroller for signal processing [22]. The main characteristics are indicated in Tab. 3.

Table 3.

Technical characteristics of the three-component magnetometer with sensitive elements HMC1001 type

Range of magnetic induction measurements	$\pm 200 \mu\text{T}$
Frequency of issuing signals	1 – 100 Hz
Resolution	$\pm 0,0005 \mu\text{T}$
Measurement noise (3σ)	$< 0,001 \mu\text{T}$
Dimensionality of output signals	μT (nT)

Star sensor.ST400 - star sensor developed by Berlin Space Technologies in collaboration with Hyperionics Technologies [18]. This star sensor is a stand-alone solution for probing stars for complex microsatellite missions. The device has a space heritage and has been certified according to the highest standards.

Several T400s can be connected to form a backup configuration. The main ST400 characteristics are indicated in Table 4.

Table 4.

Technical characteristics of the ST400

Supply	3.7-5V DC
Power Consumption	670mW 3.7V
Dimension (ST400D) /with Baffle 40 Sun Exclusion	48x57x89mm ³ /74x74x146mm ³
Mass (ST400D) /with Baffle 40 Sun Exclusion	270g / 350g
Operation Temperature	-20°C to +40°C
Accuracy (pitch & yaw) /roll	5 arcsec (1σ) /40 arcsec (1σ)
Update Rate	Up to 5Hz

Algorithm of operation of the star sensor is similarly the algorithm of operation of the Sun sensor.

Algorithm of the system orientation

To determine the orientation of the satellite, we must have the following information:

Satellite coordinates φ , λ , r (latitude, longitude and orbital radius) from the satellite navigation system (GNSS) in the Earth's geocentric coordinate system (ECEF) $X_e Y_e Z_e$ (Fig. 2).

Projections of the EMF induction vector from magnetometers in BCS (Fig. 5)

$$B_b = [B_{xb} B_{yb} B_{zb}]^T.$$

Projections of the Sun vector (the unit vector of the direction to the Sun) from the Sun sensor in the BCS

$$S_b = [S_{xb} S_{yb} S_{zb}]^T. \quad (11)$$

Based on information from GNSS, we calculate the components EMF in OGSC (Fig. 4)

$$\vec{B}_g = [B_{xg} B_{yg} B_{zg}]^T. \quad (12)$$

The components of the unit vector of the Sun, calculated in ECI according to (6), are transform into OGSC using the equation (1), (4):

$$S_g = [S_{xg} S_{yg} S_{zg}]^T = C_3 C_1^T [S_{xi} S_{yi} S_{zi}]^T. \quad (13)$$

When using star sensors, we will get projections of unit vectors of detected stars from the star sensor in BCS similarly (11)

$$K_b = [K_{xb} \ K_{yb} \ K_{zb}]^T. \quad (14)$$

The components of the unit vectors of recognized stars from the catalog of the starry sky (8) are transferred to OGSC in the same way as (13)

$$[K_{xg} \ K_{yg} \ K_{zg}]^T = C_3 C_1 [K_{xi} \ K_{yi} \ K_{zi}]^T. \quad (15)$$

The TRIAD method of satellite orientation determination. According to this method [23], we will build triads - coordinate systems from unit vectors. In OGSC we find unit vectors

$$\begin{aligned} \vec{b}_g &= \vec{B}_g / B_g, \quad B_g = (B_{xg}^2 + B_{yg}^2 + B_{zg}^2)^{1/2}, \quad \vec{s}_g = \vec{S}_g / S_g, \\ S_g &= (S_{xg}^2 + S_{yg}^2 + S_{zg}^2)^{1/2}. \end{aligned}$$

We find the vector product from the unit vectors $\vec{b}_1 = \vec{B}_g \times \vec{S}_g$ and its unit vector $\vec{m}_1 = \vec{b}_1 / b_1$. We get a double vector multiplication $\vec{n}_1 = \vec{B}_g \times \vec{m}_1$.

The same vectors can be found in LCS: $\vec{b}_b = \vec{B}_b / B_b$, $\vec{s}_b = \vec{S}_b / S_b$, vector multiplication $\vec{b}_2 = \vec{b}_b \times \vec{s}_b$ and its ort $\vec{m}_2 = \vec{b}_2 / b_2$, a double vector multiplication $\vec{n}_2 = \vec{b}_b \times \vec{m}_2$.

We form matrices $M_g = [\vec{b}_g \ \vec{m}_1 \ \vec{n}_1]$, $M_b = [\vec{b}_b \ \vec{m}_2 \ \vec{n}_2]$, from which we find the matrix of direction cosines between coordinate systems OGSC and BCS

$$C^{bg} = M_b \cdot M_g^{-1}. \quad (16)$$

For an orthogonal matrix M_g we have: $M_g^{-1} = M_g^T$.

Matrix (16) is the direction cosines matrix of LCS in OGCS, from which we can find satellite orientation angles:

$$\psi = -\arctan\left(\frac{c_{13}^{bg}}{c_{11}^{bh}}\right), \quad \gamma = -\arctan\left(\frac{c_{32}^{bg}}{c_{22}^{bh}}\right), \quad \vartheta = -\arctan\left(\frac{c_{13}^{bg}}{\sqrt{(c_{11}^{bh})^2 + (c_{12}^{bh})^2}}\right) \quad (17)$$

The orientation of the satellite can also happened in the orbital satellite coordinate system (OSCS). Then the matrix of guiding cosines between BCS and OSCS will find as follows:

$$C^{bo} = C_2 C^{bg} \cdot C^{bo} = C_2 C^{bg}. \quad (18)$$

When using the star sensors in expressions (16), (17), we will use the projections of the unit vectors of recognized stars from the star sensor (14) and (15) in the BCS similarly to expressions (11), (13).

Conclusions

The methodology and algorithms for determining the orientation of a micro and nano satellite relative to the orbital geographic coordinate system (yaw, pitch and roll angles) using measurements by onboard sensors and calculating the induction vectors of the Earth's magnetic field and the direction to celestial bodies are shown. The procedure for using the triad method for calculating satellite orientation angles is described. The technical means that allow to use the given method of determining the orientation on small satellites of the CubeSat class are shown.

References

1. Silani E. Magnetic spacecraft attitude control: a survey and some new results/ E. Silani, M. Lovera // *Control Engineering Practice*. – 2005. – vol. 13. – no. 3, p. 357–371.
2. Ovchinnikov M. Y. A survey on active magnetic attitude control algorithms for small satellites / M. Y. Ovchinnikov, D. S. Roldugin // *Progress in Aerospace Sciences*. – 2019. – Vol. 109.
3. Guelman M. et al. Design and testing of magnetic controllers for Satellite stabilization // *Acta Astronaut*. 2005. – Vol. 56. – № 1–2. – P. 231–239.
4. Guo J. In-orbit results of Delfi-n3Xt: Lessons learned and move forward / J. Guo, J. Bouwmeester, E. Gill // *Acta Astronaut*. 2016. – Vol. 121. – p. 39–50.
5. Candini G. P. Miniaturized attitude control system for nanosatellites/ G. P. Candini, F. Piergentili, F. Santoni // *Acta Astronaut*. – 2012. – Vol. 81. – № 1. p. 325–334.
6. Cheng Y. QUEST and the anti-QUEST: good and evil attitude estimation introduction: QUEST/ Y. Cheng, M. D. Shuster // *Adv. Astronaut. Sci.* – 2005. – Vol. 53. – № 3. – p. 337–351.
7. Yefimenko N. V. Magnetic attitude control and stabilizing system of Egyptsat-1 spacecraft // *J. Autom. Inf. Sci.* – 2010. – Vol. 42. – № 11. – p. 64–70.
8. Searcy J. D. Magnetometer-only attitude determination using novel two-step Kalman filter approach / J. D. Searcy, H. J. Pernicka // *J. Guid. Control. Dyn.* – 2012. – Vol. 35. – № 6. – p. 1693–1701.
9. Zharov V. Spherical astronomy// Fryazino: OOO "Vek-2", 2006. – 474 p.

10. Zbrutsky O. V. The Earth remote sensing spacecraft navigation by surveying the Earth's surface / O. V. Zbrutsky, A. P. Ganja. – Kyiv: Igor Sikorsky Kyiv Polytechnic Institute, 2011. – 161 p.
11. Department of defense world geodetic system 1984. Its Definition and Relationships with Local Geodetic Systems. NIMA TR8350.2. AMENDMENT 1.3 – VA: US Government printing office, 1991. – 175 p. (Second Edition).
12. World Geodetic System — 1984 (WGS-84). Manual. // International Civil Aviation Organization. – 2002. – 138 p.
13. Montenbruck O. Astronomy on the Personal Computer / O. Montenbruck, T. Pflieger. – Springer Berlin, Heidelberg, 2022. – 300p; 4th edition.
14. Standart of Fundamental Astronomy (SOFA) [Електронний ресурс] // 18th release. – 2021. – Режим доступу до ресурсу: <https://www.iausofa.org/>.
15. MIL-PRF-89500B. Performance specification World Magnetic Model(WMM) – US: Departments and Agencies of the Department of Defense, 2019. – 24 p.
16. The US/UK World Magnetic Model for 2020-2025, NOAA: [Електронний ресурс] – Режим доступу до ресурсу: <https://core.ac.uk/download/pdf/323304771.pdf>.
17. Meleshko V. Orientation of objects in the Earth's magnetic field. Textbook / A. Odintsov, V. Meleshko, S. Sharov// Kyiv.: Korniychuk, 2008. – 142 p.
18. SED16 Autonomous Star Sensor product line in flight results, new developments and improvements in progress / [L. Blarre, D. Piot, P. Jacob and all]. – San Francisco: AIAA Guidance, Navigation and Control Conference and Exhibit, 2005. – (AIAA 2005–5930).
19. ACH-5206 GPS/GALILEO/GLONASS/SBAS receiver module Data sheet. – Ukraine, Smila: kbcentr, 2019. – 21 p. – (AEAO.468173.002_v.0).
20. NanoSSOC-A60 Sun Sensor for Nano-Satellites Analog interface Technical Specification, Interfaces & Operation. – Sevilla, Spain : Solar MEMS Technologies S.L., 2020. – p. 5–6.
21. Stephen A. Autonomous Sun-Direction Estimation Using Partially Under-determined Coarse Sun Sensor Configurations / A. Stephen, O'Keefe. – M.S.: University of Colorado, Department of Aerospace Engineering Sciences, 2015. – p. 41-43.
22. Honeywell HMC/1002/1021/1022 Technical Specifications. –Honeywell Aerospace, 2019. – p. 1–8.
23. Melashchenko O. Analysis of the determination algorithms for the designation of orientation / O. Melashchenko, L. Rizhkov, D. Stepurenko // Mechanics of gyroscopic systems. – № 21. – 2011. – p. 44–57.